Application of Storm Surge and Tsunami Simulator in Oceans and Coastal Areas (STOC) to Tsunami Analysis

by

Takashi Tomita[1], Kazuhiko Honda[2] and Taro Kakinuma[3]

ABSTRACT

The numerical simulator named STOC (Storm surge and Tsunami simulator in Oceans and Coastal areas) has been developed to estimate the damages by tsunamis and storm surge. It includes non-hydrostatic and three-dimensional models of STOC-IC and STOC-VF to estimate the flow velocity and wave force of tsunamis. In this study, STOC was applied to tsunami analysis; especially, the sub-model of STOC-IC that adopted the vertically-integrated continuity equation to determine the free water surface was verified in comparison with the physical model experiments in which the tsunami reduction around an opening section of breakwaters, tsunami transformation on a slope and tsunami wave forces were investigated. The non-hydrostatic model, STOC-IC, was able to estimate the tsunami reduction by structures with the use of the suitable eddy viscosity model, and calculate tsunami wave pressure on a vertical wall in the fine computational grid whose size was a few meters in real scale.

KEYWORDS: Numerical Simulation, Three Dimensional Model, Tsunami, Tsunami Flow, Tsunami Wave Pressure

1. INTRODUCTION

The Indian Ocean Tsunami on 26 December 2004 caused severe damages in many coastal areas along the Indian Ocean. Tsunami fluid motion on land was complicated depending on local topography and existence of structures. The resultant tsunami action caused various types of damage. For example, in Banda Aceh, Northern Sumatra, Indonesia, almost houses within 2-3 km of a beach were broken by the tsunami more than 4m on the ground and a large vessel whose length and width were approximately 60m and 20m respectively was floated into the land as well as small fishery boats. On the other hand, field surveys on the tsunami damages showed that some structures such as breakwaters, coastal mounds, rigid houses etc. were effective in reduction of tsunami momentum behind them. As shown in Picture 1, a high mound, which was a road connecting to a bridge, reduced the destruction of the first floor of a shop against the 10 m tsunami. To understand and estimate these tsunami damages and to consider suitable measures for the reduction of damages, it is necessary to estimate fluid velocity and wave pressure of tsunami as well as inundation area and its water depth.

Picture 1 Reduction of tsunami damage by a road mound in Banda Aceh

In general, tsunamis can be estimated by horizontally two-dimensional numerical model with the use of the hydrostatic pressure assumption, because the tsunamis are extreme long waves. However, Fujima et al. [1] showed that the tsunamis had non-hydrostatic feature around an opening section of breakwaters in which a submerged breakwater was installed

[1] Tsunami Research Director, Tsunami Research Center, Port and Airport Research Institute, Yokosuka, Kanagawa 239-0826 Japan

[2] Project Researcher, Tsunami Research Center,, ditto

[3] Special Researcher, Littoral Drift Division, Marine Environment and Engineering Department, ditto

and non-hydrostatic numerical model calculated such a behavior accurately. Yoneyama et al. [2] also accomplished the calculation of 30 m-runup on a v-shaped valley in the 1993 Okushiri Tsunami Disaster with the use of their non-hydrostatic model. These results suggest that the tsunamis have non-hydrostatic features depending on complicated topography and the interaction with structures and therefore the non-hydrostatic models are capable of estimating them.

In this study a numerical simulator, STOC (Storm surge and Tsunami simulator in Oceans and Coastal areas), which includes non-hydrostatic and three-dimensional fluid models, was applied to tsunami analysis and verified in comparison with some physical model experiments. Especially, the performance of a non-hydrostatic model named STOC-IC was examined.

2. NUMERICAL MODEL

2.1 Model Components

The numerical simulator, STOC, has been developed to estimate tsunami behavior including the interaction with structures such as coastal defense facilities and buildings. The simulator is a hybrid model consisting of three-dimensional and non-hydrostatic models of STOC-IC and STOC-VF and a multilevel model of STOC-ML. The discrepancy between STOC-IC and STOC-VF is in the calculation method of free water surfaces. Figure 1 shows an example of model arrangement of STOC.

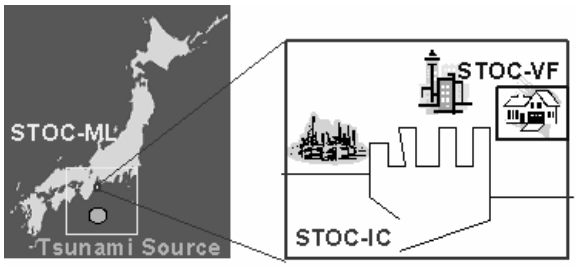

Fig. 1 Example of model arrangement of STOC

STOC-ML is the multi-level model to compute the tsunamis in a wide sea area in less computation time. In this model, the water area is vertically divided to some levels. The governing equations of the model are the continuity equation and Reynolds-averaged Navier-Stokes equations as the momentum equations, as described in Sec 2.2. Instead of calculation of the vertical momentum equation, the hydrostatic pressure is computed, since the assumption of hydrostatic is applied in each level.

STOC-IC is the non-hydrostatic pressure model in three-dimensions to estimate tsunamis in a wide area whose size is a coastal city where there are many structures and non-hydrostatic behavior of tsunami is induced by them. To reduce computational time and memory than another non-hydrostatic model of STOC-VF, STOC-IC uses the integrated continuity equation to analyze the position of free water surface and can be connected to STOC-ML. The governing equations are also the continuity equations and the Reynolds-averaged Navier-Stokes equations in three-dimensions.

STOC-VF is also the non-hydrostatic pressure model in three-dimensions. The difference of STOC-IC is in calculation of the position of the free water surface. STOC-VF adopts the method of volume of fluid (VOF) [3] to determine the free water surface in order to calculate tsunami overtopping and impulsive wave forces. It is, therefore, applied to analysis of .structural destruction by the tsunami and so on.

2.2 Governing Equations

Basic governing equations of all sub-models of STOC are the Reynolds-averaged Navier-Stokes equations and the continuity equation in three dimensions for incompressible fluids as follows:

- Reynolds averaged Navier-Stokes equations in x, y and z directions, respectively

$$\gamma_v \frac{\partial u}{\partial t} + \frac{\partial}{\partial x}\left(\gamma_x uu\right) + \frac{\partial}{\partial y}\left(\gamma_y vu\right) + \frac{\partial}{\partial z}\left(\gamma_z wu\right) - f_0 v$$
$$= -\gamma_v \frac{1}{\rho_0}\frac{\partial p}{\partial x} + \frac{\partial}{\partial x}\left(\gamma_x \nu_e 2\frac{\partial u}{\partial x}\right)$$
$$+ \frac{\partial}{\partial y}\left\{\gamma_y \nu_e\left(\frac{\partial u}{\partial y} + \frac{\partial v}{\partial x}\right)\right\} + \frac{\partial}{\partial z}\left\{\gamma_z \nu_e\left(\frac{\partial u}{\partial z} + \frac{\partial w}{\partial x}\right)\right\} \quad (1)$$

$$\gamma_v \frac{\partial v}{\partial t} + \frac{\partial}{\partial x}\left(\gamma_x uv\right) + \frac{\partial}{\partial y}\left(\gamma_y vv\right) + \frac{\partial}{\partial z}\left(\gamma_z wv\right) + f_0 u$$
$$= -\gamma_v \frac{1}{\rho_0}\frac{\partial p}{\partial y} + \frac{\partial}{\partial x}\left\{\gamma_x \nu_e\left(\frac{\partial v}{\partial x} + \frac{\partial u}{\partial y}\right)\right\} +$$
$$\frac{\partial}{\partial y}\left(\gamma_y \nu_e 2\frac{\partial v}{\partial y}\right) + \frac{\partial}{\partial z}\left\{\gamma_z \nu_e\left(\frac{\partial v}{\partial z} + \frac{\partial w}{\partial y}\right)\right\} \qquad (2)$$

$$\gamma_v \frac{\partial w}{\partial t} + \frac{\partial}{\partial x}\left(\gamma_x uw\right) + \frac{\partial}{\partial y}\left(\gamma_y vw\right) + \frac{\partial}{\partial z}\left(\gamma_z ww\right)$$
$$= -\gamma_v \frac{1}{\rho_0}\frac{\partial p}{\partial z} + \gamma_v \frac{\rho - \rho_0}{\rho_0} g +$$
$$\frac{\partial}{\partial x}\left\{\gamma_x \nu_e\left(\frac{\partial w}{\partial x} + \frac{\partial u}{\partial z}\right)\right\} + \frac{\partial}{\partial y}\left\{\gamma_y \nu_e\left(\frac{\partial w}{\partial y} + \frac{\partial v}{\partial z}\right)\right\}$$
$$+ \frac{\partial}{\partial z}\left(\gamma_z 2\frac{\partial w}{\partial z}\right) \qquad (3)$$

- Continuity equation

$$\frac{\partial}{\partial x}\left(\gamma_x u\right) + \frac{\partial}{\partial y}\left(\gamma_y v\right) + \frac{\partial}{\partial z}\left(\gamma_z w\right) = 0 \qquad (4)$$

in which (x, y, z) are the Cartesian coordinates, (u, v, w) the velocity in the directions of x, y and z, ρ the fluid density, ρ_0 a reference density, p the pressure, g the gravitational acceleration, ν_e the eddy viscosity, and f_o the Coriolis coefficient. The porosity ε and transmissivity γ_x, γ_y and γ_z in each direction of x, y and z introduced by Sakakiyama and Kajima [4] are imposed to express configurations of the sea bottom and structure faces smoothly.

In STOC-IC and STOC-ML, the free water surface is determined by the vertically integrated continuity equation:

$$\gamma_v \frac{\partial \eta}{\partial t} + \frac{\partial}{\partial x}\int_{-h}^{\eta} \gamma_x u dz + \frac{\partial}{\partial y}\int_{-h}^{\eta} \gamma_y v dz = 0 \qquad (5)$$

in which η is the free water surface elevation, and h the still water depth.

In STOC-VF, the free water surface is analyzed by the calculation of the function of volume of fluid on the water free surface.

2.3 Numerical Scheme

The governing equations are solved by the finite difference method in which a staggered mesh in space and leapfrog method in time are used. The diffusion terms are discretized with the second-order central scheme, while the advection terms are expanded with a hybrid scheme where the first-order upwind scheme is combined with the second-order central scheme for stability.

To calculate of pressure in STOC-IC and STOC-VF, the method of SMAC (Simplified Marker And Cell) [5] is applied

Connection between STOC-IC and STOC-ML is made in overlapping zones in which the physical quantities such as the water surface displacement, velocities, pressure etc. in each computational area of STOC-IC and STOC-ML are adjusted using the interpolation technique.

3. APPLICATION TO TSUNAMIS IN PHYSICAL MODEL EXPERIMENTS

3.1 Tsunami around an Opening Section of Breakwaters

The model validation of STOC was investigated in comparison with the results of physical model experiments by Tanimoto et al. [6], in which the water surface elevations of the tsunamis were measured around an opening section of breakwaters with a submerged breakwater as shown in Fig. 2.

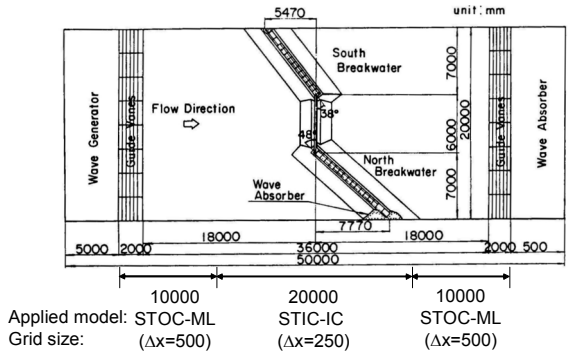

Fig. 2 Experimental basin with breakwaters

In the computations, STOC was applied in the range of 10 m in front and back of the submerged breakwater in which the size of computational grid was 0.25 m. In both sides of it STOC-ML was applied and the grid size was 0.50 m. The grid size of the transverse direction was 0.25 m in all of the computational area. The vertical grid sizes were varied so as to be fine grid near the free water surface. The tsunami in the computation was reproduced as a uniform flow whose speed was 1.00 m/s, because in the experimental cases the tsunamis were produced by uniform flows of 0.98 m/s and 1.05 m/s.

The comparison of the tsunami water surface variation in space is shown in Figure 3. In the figure, Cal. (-2, -4), for example, indicates the numerical result using the horizontal and vertical eddy viscosity coefficients of 10^{-2}m^2/s and 10^{-4}m^2/s, respectively, and Cal. (SGS) shows the numerical result with the eddy viscosity like the subgrid scale (SGS) model of in large eddy simulation (LES) as shown by (6) in the same way as Fujima et al. [1] following Nakatsuji et al. [7].

$$\nu_e = (C_s \Delta)^2 \sqrt{\left(\frac{\partial u_i}{\partial x_j} + \frac{\partial u_j}{\partial x_i}\right)\left(\frac{\partial u_i}{\partial x_j} + \frac{\partial u_j}{\partial x_i}\right)} \qquad (6)$$

in which $\Delta = (\Delta x \times \Delta y \times \Delta z)^{1/3}$ and $C_s = 0.2$ that is the ordinal value for the SGS model.

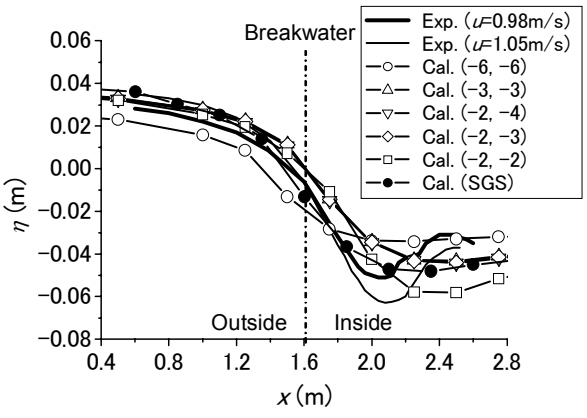

Fig. 3 Free water surface around the opening section of breakwaters

The use of eddy viscosity coefficient like SGS-type depending on spatial variation of flow provided good results in the numerical simulation by STOC-IC. However, it was necessary to investigation on the turbulent model more since the combination of STOC-IC and SGS-type eddy viscosity could not express the recovery of water surface elevation behind the breakwaters well.

3.2 Tsunami transformation on slope

Since Tsuruya and Nakano (Tanimoto et al. [8]) investigated tsunami transformation on a uniform slope (Fig. 4) experimentally, the computation results by STOC-IC were compared with their experimental results in Fig. 5. Corresponding to the experimental condition, the slope angle was 1/200 and the tsunami wave period was 40 s, and wave steepness was approximately 1.9×10^{-4} at Point H whose water depth was 1.0 m. In the computation, the dimensionless grid sizes $\Delta x/L$ and $\Delta z/H$ were 4 $\times 10^{-3}$ and 0.5, respectively, in which L was the wavelength at 1.0 m depth and H the incident wave height of 0.02 m based on the wave steepness in the experiment.

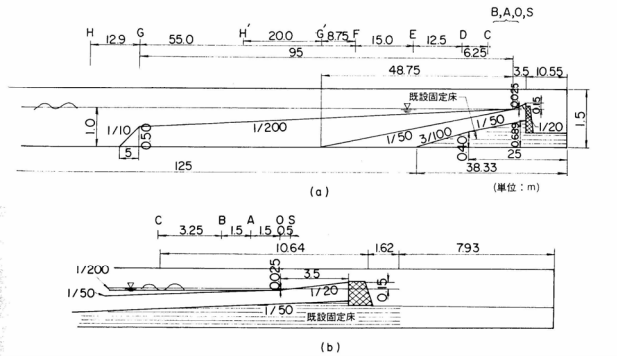

Fig. 4 Tsuruya and Nakano's experiment set up

The computed tsunami forms as a whole were quantitatively comparable with the experimental forms. However, considerably high tsunami was calculated at Point C when the second incident tsunami wave encountered with the reflected wave of the first tsunami. This discrepancy indicates that there are some improvements on

the numerical scheme to calculate the free water surface when the incident and reflected waves meet each other.

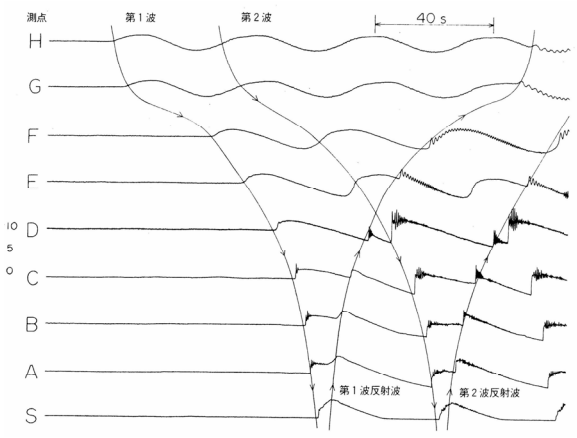

(a) Experimental result

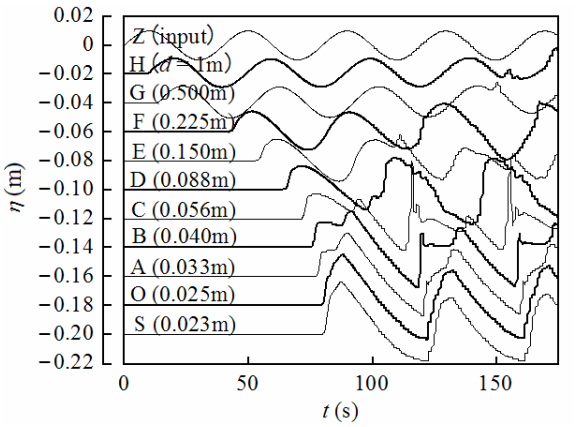

(b) Numerical result

Fig. 5 Tsunami transformation on slope

3.3 Tsunami Wave Pressure

Computed tsunami wave pressures acting on a seawall were compared to experimental results by Tanimoto et al. [8] in which the wave pressures due to the main body of tsunamis shown as P_s in Fig. 6 acting on a vertical wall on uniform slopes were analyzed.

In the time variations of the experimental tsunami wave pressures in Fig. 6, the tsunami wave pressure were categorized into three types: impulsive wave pressure, P_i, solitaly wave pressure, P_p, and wave pressure of tsunami main body, P_s. The wave pressure, P_s, is significant to investigate the stability of mass structures against tsunamis.

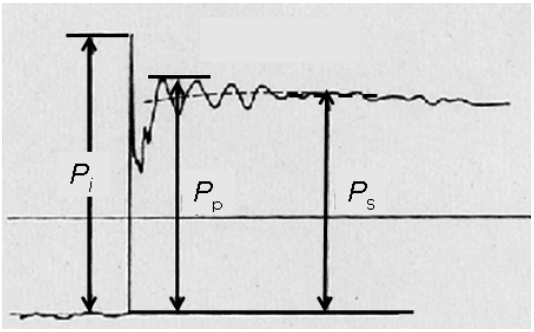

Fig. 6 Analyzed tsunami wave pressure P_s

In the computations, the tsunami wave pressure was calculated by STOC-IC, and the model topography as shown in Fig. 7 was adopted from the experimental cases.

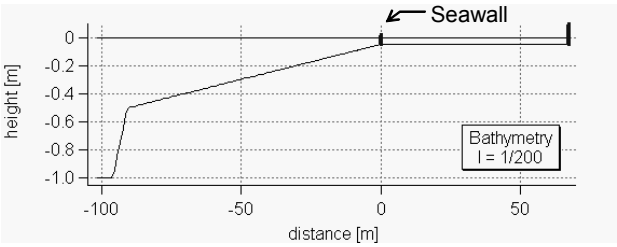

Fig. 7 Model topography to calculate tsunami wave pressure on seawall

In the computations, the computational grid sizes around the seawall were 0.01 m in the tsunami propagation direction, 0.5 m in the transverse direction, and 0.01 m in vertical direction. The time marching step was 0.002 s. If the model scale is 1/200, the grid size is 2.0 m in front of the seawall and the time step is 0.028 s.

Figure 8 shows the vertical distribution of the tsunami wave pressure, P_s, by the experimental

and numerical simulations. The data was the maximum value in each experimental and numerical run, and then did not always appear each other in the same time. The computed tsunami wave pressures were in good agreement with the experimental pressures. Moreover, the computed tsunami wave pressures were also well comparable with other experimental pressures by Ikeno et al. [9]. Therefore, it confirmed that the non-hydrostatic model of STOC-IC had performance to estimate the sustainable tsunami pressure following the impulse pressure, which might be predominant force for movement of massive structures like a breakwater.

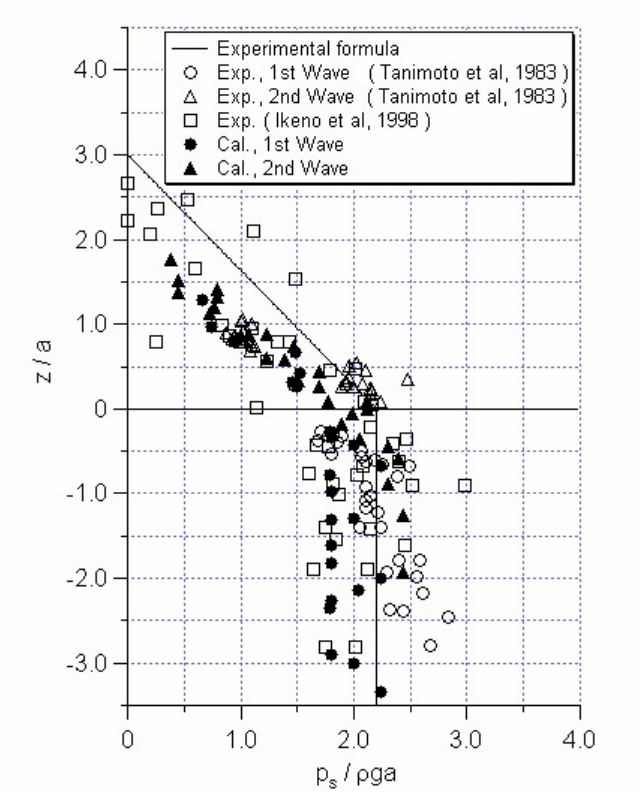

Fig. 8 Experimental and numerical tsunami wave pressures acting on a vertical wall

4. CONCLUSIONS

The main conclusions in this study are as follows:

1) The numerical tsunami simulator, STOC, was developed to estimate hydraulics and hydrodynamics of tsunami. Especially non-hydrostatic model of STOC-IC showed good performance in comparison with the hydraulic experiments.
2) The non-hydrostatic model was capable of estimating the reduction of tsunami by structures using the suitable eddy viscosity model.

In the study proceeding at present, we are going to apply the numerical simulator of STOC to real topography in order to understand what happen there by the tsunami striking under the interaction with structures and to develop "Tsunami Dynamic Hazard Map" which gives tsunami features including tsunami hydrodynamics as well as hydraulics visually to the citizens, policy makers etc. Figure 8 is an example of the numerical output which shows the tsunami flooding in an imaginary coastal city under the interaction with structures. This may be one of tsunami dynamic hazard map.

Moreover, we must modify the numerical scheme to calculate the water surface when the incident tsunami wave encounters the reflected wave of the previous tsunami wave. Considering the tsunami form in front of the seawall, the tsunami wave pressure on the seawall is also verified in point of variation in time.

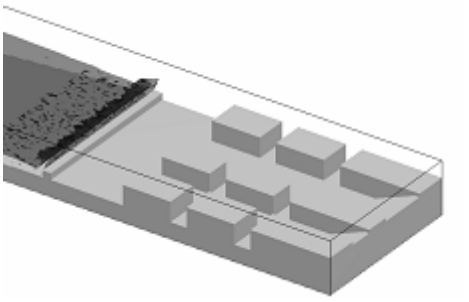

Fig. 9 Example of demonstration of tsunami flooding in a coastal city

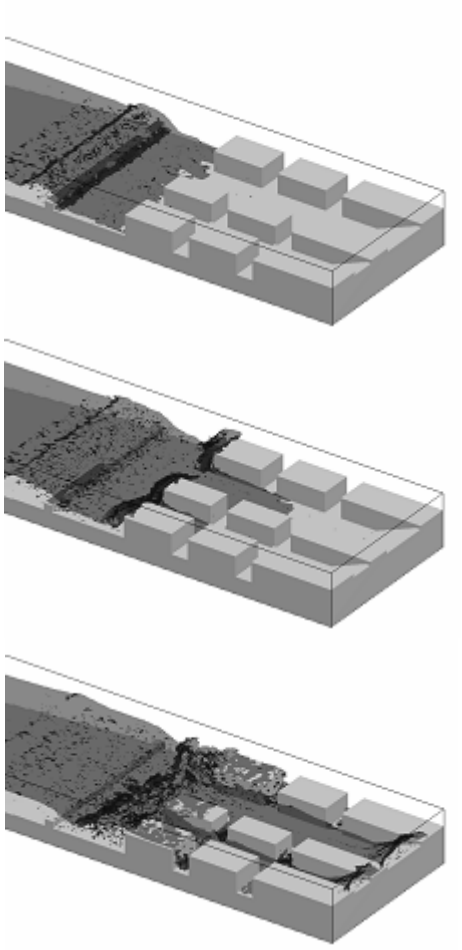

Fig. 9 (cont.) Example of demonstration of tsunami flooding in a coastal city

5. REFERENCES

1. Fujima, K. et al.: Development of the 2d/3d Hybrid Model for Tsunami Numerical Simulation, *Coastal Eng. Jour.*, 44(4), 373-397, 2002.
2. Yoneyama N., M. Matsuyama and H. Tanaka: Numerical analysis for Locally High runup of 1993 Hokkaido Nansei-Oki Seismic Tsunami, *Jour. JSCE*, 705/II-59, 139-150, 2002 (in Japanese).
3. Hirt, C. W. and B. D. Nichols: Volume of Fluid (VOF) Method for the Dynamics of Free Boundaries, *Jour. Computational Physics*, 29, 201-225, 1981.
4. Sakakiyama, T. and R. Kajima: Numerical Simulation of Nonlinear Wave Interacting with Permeable Breakwaters, *Proc. 23rd Int. Conf. Coastal Eng.*, ASCE, 1517-1530, 1992.
5. Amsden, A.A. and F.H. Harlow: A Simplified MAC technique for Incompressible Fluid Flow Calculations, *Jour. Computational Physics*, 6, 322-325, 1970.
6. Tanimoto, K et al.: Study on Stability of Submerged Dike at the Opening Section of Tsunami Protection Breakwaters, *Rep. Port and Harbour Res. Inst.*, 27(4), 93-121, 1988 (in Japanese).
7. Nakatsuji, K., S. Karino, and H. Kurita: Finite Element Analysis of Tidal Flow in the Osaka Bay with Subgrid Scale Eddy Coefficient, *Proc. Hydraulic Eng.*, JSCE, 36, 693-696, 1992 (in Japanese).
8. Tanimoto, K et al.: Field and Laboratory Investigations of the Tsunami Caused by 1983 Nihonkai Chubu Earthquake, *Tech. Note Port and Harbour Res. Inst.*, 470, 1983 (in Japanese).
9. Ikeno, M., M. Matsuyama and H. Tanaka: Shoaling and Soliton Fission of Tsunami on a Shelf and Wave Pressure for Tsunami-Resistant Design of Breakwater by Large Wave Flume-Experiments, *Proc. Coastal Eng.*, JSCE, 45, 366-370, 1998 (in Japanese).